Journal of Alloys and Compounds 509 (2011) 9959–9963

Contents lists available at ScienceDirect

Journal of Alloys and Compounds

journal homepage: www.elsevier.com/locate/jallcom

Synthesis and photoluminescence of wurtzite CdS and ZnS architectural structures via a facile solvothermal approach in mixed solvents

Xinjuan Wang[a,b,*], Bingsuo Zou[a,c,**], Qinglin Zhang[a], Aihua Lei[a], Wenjie Zhang[a], Pinyun Ren[a]

[a] State Key Lab of CBSC, Micronano Research Center, Hunan University, Changsha 410082, China
[b] Zibo Environmental Protection Bureau, Zibo 255030, China
[c] Micro-nano Technology Center and School of MSE, BIT, Beijing 100081, China

ARTICLE INFO

Article history:
Received 16 March 2011
Received in revised form 3 August 2011
Accepted 3 August 2011
Available online 10 August 2011

Keywords:
Semiconductors
Nanostructures
Solvothermal process
Optical properties

ABSTRACT

CdS and ZnS nanostructures with complex urchinlike morphology were synthesized by a facile solvothermal approach in a mixed solvent made of ethylenediamine, ethanolamine and distilled water. No extra capping agent was used in the process. The structure, morphologies and optical properties of these nanostructures were characterized by X-ray diffraction (XRD), field emission scanning electron microscopy (FE-SEM), transmission electron microscopy (TEM), and photoluminescence (PL) spectroscopy. The as-synthesized urchinlike architectures were composed of nanorods with wurtzite structure. The preferred growth direction of nanorods was found to be the [0 0 1] direction. The PL spectrum of CdS nanostructures exhibited a highly intense red emission band centered at about 706 nm. On the basis of the experimental results, a possible growth process has been discussed for the formation of the CdS and ZnS urchinlike structures.

1. Introduction

Semiconductor nanostructures, such as nanorods, nanowires, nanobelts, have attracted a great deal of attention because of their exceptional properties and promising application in optoelectronic nanodevices [1–3]. Recently, assembling these 1D semiconductor nanocrystalline into complex 3D architectures has been a crucial issue in nanoscience research. Such complex 3D architectures combining the features of nanoscale building blocks will show unique properties different from those of the monomorphological structures [4]. Thus, developing a facile and economical approach to synthesize nanomaterials with complex 3D architectures is very important to nanoscience and synthetic chemistry.

CdS and ZnS, the well-known direct and wide band-gap semiconductors, have attracted significant research interest due to their special properties and applications in nonlinear optical devices, field emitters, photodetectors, sensors, data storage, etc. [5–9]. So far, various techniques, such as laser ablation, solution-based route, thermal decomposition and evaporation [10–14], have been employed to synthesize CdS and ZnS nanostructures. CdS and ZnS nanostructures with various morphologies have been reported in the literatures [11,12,14–16], including nanoparticles, nanorods, nanowires and nanospheres. In contrast to 1D nanostructures, CdS and ZnS with complex 3D architectures exhibit much exceptional properties and excellent applications in solar cells and photocatalysis [17–19]. More recently, CdS and ZnS nanocrystals with complex architectures have been prepared by evaporation, hydrothermal and solvothermal approaches [20–24]. However, most of the methods mentioned above are complicated, or it is inevitable to use expensive capping agent. Thus, how to design and develop a simple, economic method to prepare CdS and other similar semiconductors with complex architectures is still a great challenge.

In this paper, we report a facile and economical solvothermal route to fabricate CdS and ZnS urchinlike architectures on a large scale in a mixed solvent of ethylenediamine, ethanolamine and distilled water. No extra capping agent was used in the process. To the best of our knowledge, this kind of self-assembled growth of CdS and ZnS urchinlike architectures formed in ternary solution has not been reported. A possible mechanism for the formation of CdS and ZnS urchinlike architectures in this mixed solution was proposed. The morphologies, structure and optical properties of these products were also studied.

2. Experimental

All the chemicals used were analytical grade and without further purification. In a typical procedure, 1 mmol cadmium acetate and 2 mmol thiourea were dissolved

* Corresponding author at: Micronano Research Center, Hunan University, Lushan South Road, Changsha 410082, China. Tel.: +86 010 68913948; fax: +86 010 68913938.
** Corresponding author at: Micro-nano Technology Center and School of MSE, BIT, Beijing 100081, China. Tel.: +86 010 68913948; fax: +86 010 68913938.
E-mail addresses: wangxj@hnu.edu.cn (X. Wang), zoubs@bit.edu.cn (B. Zou).

0925-8388/$ – see front matter © 2011 Elsevier B.V. All rights reserved.
doi:10.1016/j.jallcom.2011.08.001

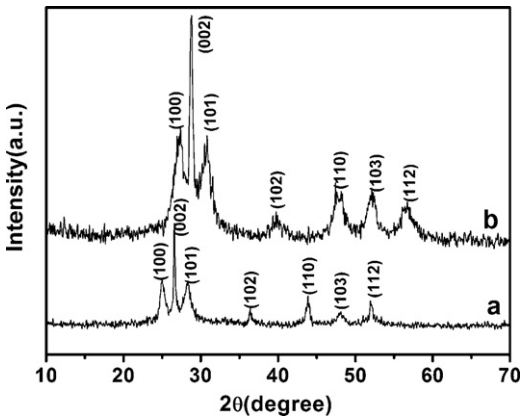

Fig. 1. XRD patterns of: (a) CdS; (b) ZnS.

in a given amount of distilled water and the mixture was dispersed to form a homogeneous solution by constant strong stirring. Then, a given amount of ethanolamine (EA) and ethylenediamine (EN) were added to the cadmium acetate solution at room temperature. After 10 min stirring the mixture was transferred into a Teflon-lined stainless autoclave (50 mL capacity). The autoclave was sealed and maintained at 180 °C for 24 h, and then cooled to ambient temperature naturally. The final yellow product was collected and washed with distilled water and absolute alcohol for several times and dried in a vacuum oven at 60 °C. The ZnS was prepared by the same method with CdS. Differently, the reactant is zinc acetate and the colour of the product is white.

The crystal structure of the as-prepared samples was studied using a Bruker D8 X-ray diffractometer with Cu Kα irradiation at λ = 1.5406 Å. The morphology and composition of the products were observed on a Hitachi S-4800 field-emission scanning electron microscopy (FE-SEM) and high resolution transmission electron microscopy (HR-TEM, JEOL-3010), which they equipped with energy-dispersive X-ray (EDS) analyzers. Room temperature photoluminescence (PL) was recorded on Alpha (WITec, Germany) near-field scanning optical microscope (NSOM) system from RHK Technology using the Ar^+ laser (488 nm) and He–Cd laser (325 nm) as the excitation source.

3. Results and discussion

The powder XRD patterns of the as-prepared products are shown in Fig. 1. Fig. 1a shows the X-ray diffraction pattern of as-prepared CdS nanostructures. The strong and sharp diffraction peaks indicated that the sample is well crystallized. All the diffraction peaks can be indexed as wurtzite CdS with lattice constant of $a = b = 4.136$ Å and $c = 6.713$ Å, which are in good agreement with the literature values (JCPDS Card No. 77-2306). ZnS sample has the similar XRD pattern to CdS. Fig. 1b shows that all the diffraction peaks of ZnS can be indexed as wurtzite ZnS with lattice constants $a = 3.82$ Å and $c = 6.26$ Å, which match well with the standard card (JCPDS Card No. 36-1450). No peaks of impurities were detected, revealing the high purity of the as-synthesized products. The FTIR analysis showed that there were no obvious infrared characteristic absorption peaks of the organic functional groups in the infrared spectra of our samples. Compared to the standard reflection, the intensity of the (0 0 2) diffraction peak of both samples is comparatively strong, which indicates the preferential crystal growth orientation along the *c*-axis. Fig. 2 shows the EDS pattern of the as-prepared products. In Fig. 2a, it shows only the peaks for Cd, S and Cu. The observed Cd and S peaks arise from the sample while the Cu peaks arise from copper grid, indicating the purity of CdS sample. The atomic ratio of Cd and S is up to about 1.10. Similar observations are noticed from the EDS pattern recorded for ZnS sample, as shown in Fig. 2b. Elemental analysis reveals that the products contain only Zn and S with a stoichiometric ratio of 27:23.

Fig. 3 shows the typical FE-SEM images of the as-prepared products. FE-SEM observation shown in Fig. 3a reveals that the as-prepared CdS products consist of a large quantity of urchin-like architectures with diameters in the range of 0.5–1 μm. These urchinlike architectures have no obvious region between each other, and most of them are interconnected together. High-magnification FE-SEM image inserted in the upper right of Fig. 3a clearly reveals that the urchinlike architectures are constructed from the assembly of nanorods. The diameter of nanorods is around 25 nm. Most of the nanorods have smooth surfaces. The size and shape of the urchinlike CdS nanostructures strongly depend on the volume ratio of the mixed solvents. Fig. 3b shows the FE-SEM image of the CdS product obtained with the volume ratios of V_{EN}:V_{EA}:V_{water} of 1:1:1. Urchinlike nanostructures with diameter of about 300 nm are observed. Upon close examination of the nanostructures presented in the upper right of Fig. 3b, it is clear that the diameter of the nanorods becomes smaller and the surface of the nanorods becomes rough. Fig. 3(c and d) shows the FE-SEM image of ZnS products. A panoramic morphology of the product is presented in Fig. 3c, indicating the high yield and uniformity. The enlarged image in Fig. 3d clearly reveals that the obtained ZnS, with diameters in the range of 0.5–1.5 μm, exhibits the well-defined urchinlike structure constructed from tightly self-assembled ZnS nanorods. Therefore, ZnS nanostructures with urchinlike morphologies can also be synthesized in a similar mixed solvent by a solvothermal process, indicating the universality and versatility of this reaction medium for controlling the morphology of a family of semiconductor nanostructures.

Fig. 4 shows the typical TEM and HR-TEM images of the as-prepared products. The low-magnification image (Fig. 4a) shows that all CdS urchinlike architectures are constructed by radial nanorods arrays from center to the surface of spheres, which is in good agreement with the results from FE-SEM observations. Close

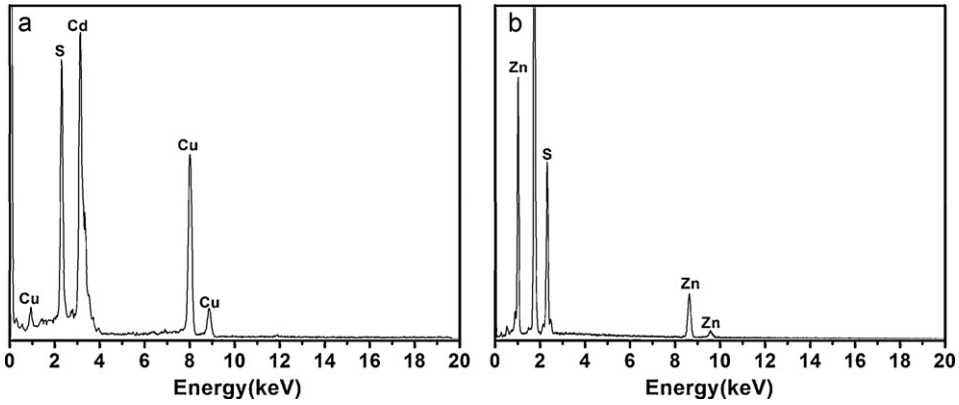

Fig. 2. EDS patterns of: (a) CdS; (b) ZnS.

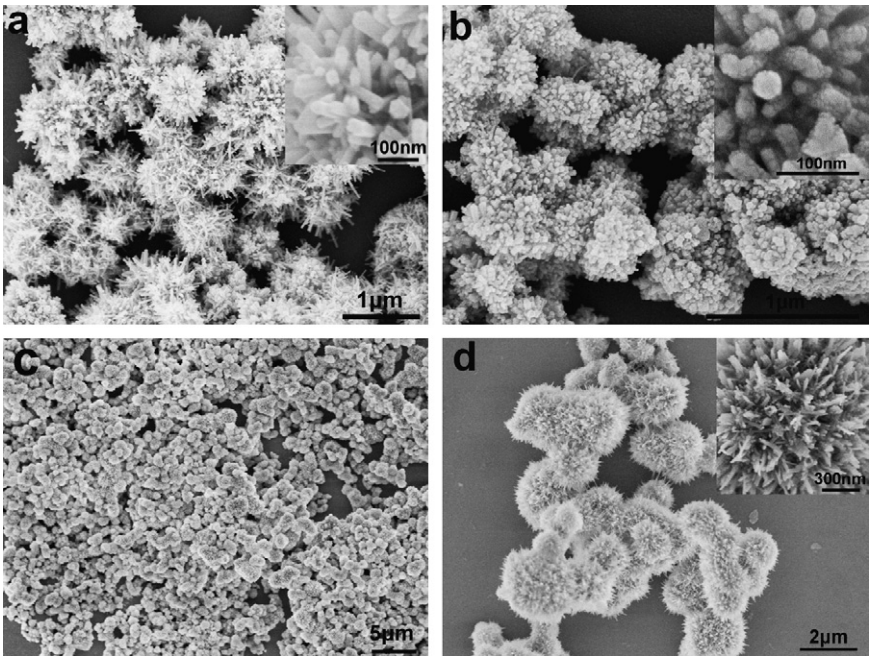

Fig. 3. FE-SEM images of as-prepared products prepared in mixed solvents: (a) CdS with volume ratios V_{EN}:V_{EA}:V_{water} = 1:5:2; (b) CdS with volume ratios V_{EN}:V_{EA}:V_{water} = 1:1:1; (c and d) ZnS with volume ratios V_{EN}:V_{EA}:V_{water} = 1:5:2.

examination of the image of Fig. 4b shows that the length of the constituent nanorods is 200–300 nm. The HR-TEM image of an individual nanorod is shown in Fig. 4c. This image displays clear lattice fringes and reveals the single crystalline nature of the rods. The measured lattice spacing is about 0.336 nm corresponding to the spacing for the (0 0 2) planes of wurtzite CdS and the preferential [0 0 1] growth direction. Fig. 4(d and e) shows the TEM image of the ZnS, which further confirms that the as-prepared ZnS nanostructures have urchinlike architectures similar to that of CdS. The HR-TEM image of an individual ZnS nanorod shows clear lattice fringes with inter-planar distances of 0.313 nm, which reveals that the nanorod is also single crystalline in nature and grows preferentially along the [0 0 1] direction.

Based on the above analysis, a possible formation mechanism of MS (M = Cd, Zn) urchinlike architectures in this mixed solvents is proposed as follows:

$$M^{2+} + xEN \leftrightarrow [M(EN)_x]^{2+} \quad (1)$$

$$M^{2+} + yEA \leftrightarrow [M(EA)_y]^{2+} \quad (2)$$

$$(NH_2)_2CS + 2OH^- \leftrightarrow CH_2N_2 + 2H_2O + S^{2-} \quad (3)$$

$$M^{2+} + S^{2-} \leftrightarrow MS \downarrow \quad (4)$$

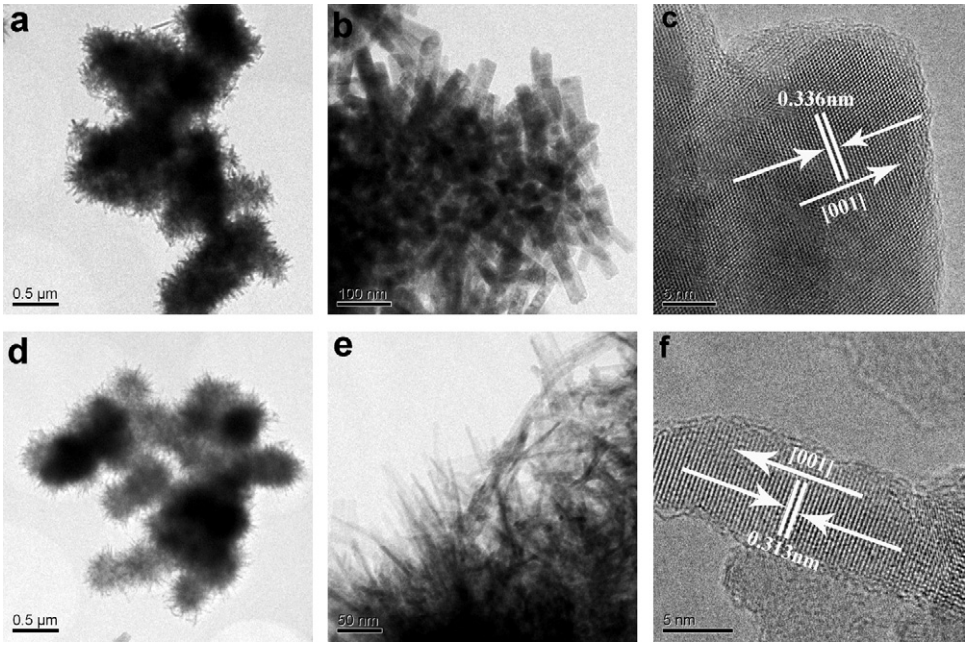

Fig. 4. (a, b, d and e) TEM and (c and f) HR-TEM images of as-prepared products: (a–c) CdS; (d–f) ZnS.

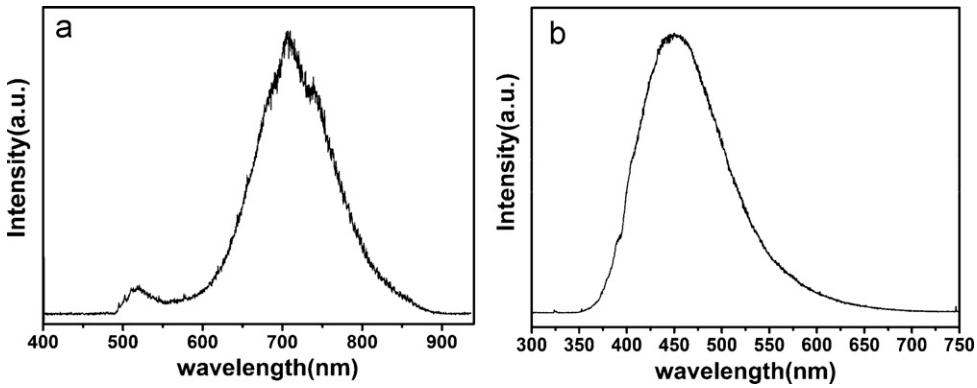

Fig. 5. Room temperature PL spectra of the as-prepared products: (a) CdS, using the Ar^+ laser (488 nm) as the excitation source; (b) ZnS, using a He/Cd laser (325 nm) as the excitation source.

Prior to the solvothermal process, the M source was mostly in the form of $[M(EN)_x]^{2+}$ and $[M(EA)_y]^{2+}$ ions, while the remaining M source existed in the form of M^{2+} ions (Reactions (1) and (2)). This is beneficial to control the concentration of the M^{2+} ions in the reaction mixture. When the precursor solution is heated, the thiourea decomposes to generate S^{2-} ions slowly and homogeneously (Reaction (3)) [25]. The S^{2-} ions will next react with the M^{2+} ions to form MS, as described by Reaction (4). When the concentration of MS has reached supersaturation, MS crystal nuclei form and then grow according to the growth habit of MS crystals. The growth habit of crystals is affected by the internal structure of a given crystal as well as external condition such as solvent [26]. In the present research, we use the mixture of ethylenediamine, ethanolamine and distilled water as reaction solvents, and keep the reaction temperature and time unchanged. Due to the use of ethylenediamine which was a structure-directing agent [27], the growth rate of the hexagonal structure of MS along the *c* axis is usually the fastest and the rodlike main core was formed selectively [28]. Subsequently, ethanolamine with two functional groups of –OH and $–NH_2$, a good oriented-assembly agent, could assemble these rodlike main cores together [29,30]. Finally, MS nanostructures with urchinlike morphology are formed. Thus, the urchinlike morphology of the MS nanostructures constructed from the assembly of nanorods is dominated mainly by the combined effect of ethylenediamine and ethanolamine.

Fig. 5 shows the room temperature photoluminescence (PL) spectra of the as-prepared products. Fig. 5a is the PL spectrum of CdS. This PL spectrum exited with 488 nm laser shows a weak emission centered at 518 nm and a strong broad emission band with the center of 706 nm. The weak emission at 518 nm belongs to the band-to-band emission [31]. The strong broad band, from 600 to 900 nm with a center around 706 nm, may arise from trap state emissions related to surface defects of CdS, in agreement with the previously report for a red emission band of CdS nanowires [32] and flowerlike CdS [28]. Fig. 5b is the PL spectrum of ZnS. It shows two emission bands. One is a strong broad blue emission centered at about 445 nm. The other is a weak emission band at about 390 nm. It is established that the emission bands centered at 390 and 450 nm are attributed to the stoichiometric vacancies (defect states) or interstitial impurities, possibly at surface of the sample [33,34].

4. Conclusions

In the present work, a facile mixed solvothermal route was designed to synthesize CdS and ZnS nanostructures with complex urchinlike morphology in a solution made of ethylenediamine, ethanolamine and distilled water. These urchinlike architectures were composed of arranged nanorods. XRD pattern and HR-TEM analysis confirm that the as-prepared products have good crystallinity with wurtzite structure. The present research shows that the combined effect of ethylenediamine and ethanolamine play an important role in determining the product morphology. The PL spectrum of the CdS displays a very strong red emission band centered at about 706 nm, while the PL spectrum of the ZnS show a strong blue emission band at around 445 nm. These complex 3D CdS and ZnS urchinlike architectures may have potential application in optics and catalysts. The facile and economical mixed solvothermal approach discussed in the present work has promise for extension to fabrication of other metal sulfide.

Acknowledgement

We thank the financial supports of National Natural Science Foundation of China (Grant Nos. 90606001, and 20873039).

References

[1] T. Zhai, L. Li, X. Wang, X. Fang, Y. Bando, D. Golberg, Adv. Funct. Mater. 20 (2010) 4233–4248.
[2] J. Jie, W. Zhang, I. Bello, C.S. Lee, S.T. Lee, Nano Today 5 (2010) 313–336.
[3] J. Chun, J. Lee, Eur. J. Inorg. Chem. 2010 (2010) 4251–4263.
[4] M. Salavati-Niasari, F. Davar, M.R. Loghman-Estarki, J. Alloys Compd. 481 (2009) 776–780.
[5] V.S. Muthukumar, J. Reppert, C.S.S. Sandeep, S.S.R. Krishnan, R. Podila, N. Kuthirummal, S.S.S. Sai, K. Venkataramaniah, R. Philip, A.M. Rao, Opt. Commun. 283 (2010) 4104–4107.
[6] X. Fang, T. Zhai, U.K. Gautam, L. Li, L. Wu, Y. Bando, D. Golberg, Prog. Mater. Sci. 56 (2011) 175–287.
[7] L. Li, P. Wu, X. Fang, T. Zhai, L. Dai, M. Liao, Y. Koide, H. Wang, Y. Bando, D. Golberg, Adv. Mater. 22 (2010) 3161–3165.
[8] X. Fang, Y. Bando, M. Liao, T. Zhai, U.K. Gautam, L. Li, Y. Koide, D. Golberg, Adv. Funct. Mater. 20 (2010) 500–508.
[9] P. Kumbhakar, M. Chattopadhyay, A.K. Mitra, Int. J. Nanosci. 10 (2011) 177–180.
[10] M. Sanz, M. LÓpez-Arias, J.F. Marco, R. Nalda, S. Amoruso, G. Ausanio, S. Lettieri, R. Bruzzese, X. Wang, M. Castillejo, J. Phys. Chem. C 115 (2011) 3203–3211.
[11] K. Li, Q. Wang, X. Cheng, T. Lv, T. Ying, J. Alloys Compd. 504 (2010) L31–L35.
[12] M. Salavati-Niasari, F. Davara, M.R. Loghman-Estarki, J. Alloys Compd. 494 (2010) 199–204.
[13] X. Chen, C.-S. Lee, X.-M. Meng, W.-J. Zhang, Mater. Lett. 65 (2011) 2585–2588.
[14] G. Dai, Q. Wan, C. Zhou, M. Yan, Q. Zhang, B. Zou, Chem. Phys. Lett. 497 (2010) 85–88.
[15] J.F.A. Oliveira, T.M. Milão, V.D. Araújo, M.L. Moreira, E. Longo, M.I.B. Bernardi, J. Alloys Compd. 509 (2011) 6880–6883.
[16] Y. Liang, H. Xu, S.K. Hark, J. Phys. Chem. C 114 (2010) 8343–8347.
[17] J.K. Dongre, M. Ramrakhiani, J. Alloys Compd. 487 (2009) 653–658.
[18] C. Wang, Y. Ao, P. Wang, J. Hou, J. Qian, S. Zhang, Mater. Lett. 64 (2010) 439–441.
[19] X. Yu, J. Yu, B. Cheng, B. Huang, Chem. Eur. J. 15 (2009) 6731–6739.
[20] Z.-X. Yang, W. Zhong, Y. Deng, C.-T. Au, Y.-W. Du, Cryst. Growth Des. 11 (2011) 2172–2176.
[21] Z.G. Chen, L. Cheng, H.Y. Xu, J.Z. Liu, J. Zou, Adv. Mater. 22 (2010) 2376–2380.
[22] W. Qiu, M. Xu, X. Yang, F. Chen, Y. Nan, H. Chen, J. Alloys Compd. 509 (2011) 8413–8420.
[23] X. Wang, Z. Feng, D. Fan, F. Fan, C. Li, Cryst. Growth Des. 10 (2010) 5312–5318.
[24] X. Wu, K.W. Li, H. Wang, J. Alloys Compd. 487 (2009) 537–544.

[25] C. Cheng, G. Xu, H. Zhang, J. Cao, P. Jiao, X. Wang, Mater. Lett. 60 (2006) 3561–3564.
[26] H. Chu, X. Li, G. Chen, W. Zhou, Y. Zhang, Z. Jin, J. Xu, Y. Li, Cryst. Growth Des. 5 (2005) 1801–1806.
[27] S. Xiong, B. Xi, C. Wang, G. Zou, L. Fei, W. Wang, Y. Qian, Chem. Eur. J. 13 (2007) 3076–3081.
[28] H. Zhang, D. Yang, X. Ma, Mater. Lett. 61 (2007) 3507–3510.
[29] S. Xiong, B. Xi, C. Wang, D. Xu, X. Feng, Z. Zhu, Y. Qian, Adv. Funct. Mater. 17 (2007) 2728–2738.
[30] X. Wang, Q. Zhang, Q. Wan, G. Dai, C. Zhou, B. Zou, J. Phys. Chem. C 115 (2011) 2769–2775.
[31] Z.Q. Wang, J.F. Gong, J.H. Duan, H.B. Huang, S.G. Yang, X.N. Zhao, R. Zhang, Y.W. Du, Appl. Phys. Lett. 89 (2006) 033102.
[32] F. Gao, Q. Lu, Nanoscale Res. Lett. 4 (2009) 371–376.
[33] A. Goudarzi, G.M. Aval, S.S. Park, M.Ch. Choi, R. Sahraei, M.H. Ullah, A. Avane, C.S. Ha, Chem. Mater. 21 (2009) 2375–2385.
[34] S. Biswas, S. Kar, S. Chaudhuri, J. Phys. Chem. B 109 (2005) 17526–17530.